Solar Energy Materials & Solar Cells 130 (2014) 364–374

Contents lists available at ScienceDirect

Solar Energy Materials & Solar Cells

journal homepage: www.elsevier.com/locate/solmat

Review

Experimental review of series resistance determination methods for III–V concentrator solar cells

G.M.M.W. Bissels *, M.A.H. Asselbergs, J.M. Dickhout, E.J. Haverkamp, P. Mulder, G.J. Bauhuis, E. Vlieg, J.J. Schermer

Radboud University Nijmegen, Institute for Molecules and Materials, Heyendaalseweg 135, 6525 AJ Nijmegen, The Netherlands

ARTICLE INFO

Article history:
Received 9 February 2014
Received in revised form
8 July 2014
Accepted 10 July 2014
Available online 12 August 2014

Keywords:
Series resistance
Review
Concentrator solar cell
CPV
III–V

ABSTRACT

Fourteen solar cell series resistance determination methods are tested for their ability to experimentally determine the series resistance of a III–V concentrator solar cell. For this purpose the series resistance is determined for a range of concentration ratios, the precision is measured and the accuracy by which a known additional resistance can be determined is tested. Only five of the methods perform adequately, but even these should be applied with care since they are either very sensitive to changes in cell temperature or only perform well at relatively high concentration ratios. None of the best values obtained with these five methods deviates more than 3.0 mΩ from their weighted average of 26.0 mΩ. The methods of Wolf & Rauschenbach and Aberle et al. were found to perform the best. It would, therefore, be preferable if the International Electrotechnical Commission adopted one of these methods as its series resistance determination standard, instead of its current method which is that of Swanson. Several methods that require only a single *IV*-curve to determine the series resistance are suitable to determine relative series resistance values.

Contents

1. Introduction

One way to significantly reduce the price of photovoltaic energy is to incorporate high efficiency solar cells into concentrator systems.

* Corresponding author. Tel.: +31 24 3653432.
E-mail address: G.Bissels@science.ru.nl (G.M.M.W. Bissels).

http://dx.doi.org/10.1016/j.solmat.2014.07.014
0927-0248/

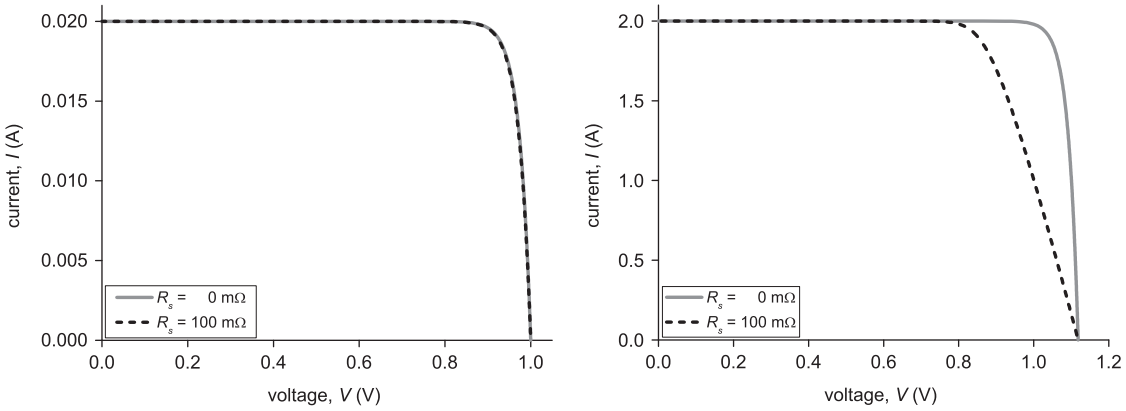

Fig. 1. Theoretical effect of a 100 mΩ series resistance on a solar cell's *IV*-curve at a light induced current of 20 mA (left) and 2 A (right).

The extreme conditions under which the cell has to perform in such a device put special requirements on the solar cell design, however. One such requirement is extra attention to a low series resistance since the associated ohmic losses increase quadratically with concentration ratio. The theoretical difference in series resistance effects between low and high concentration is illustrated in Fig. 1.

The ohmic loss between a point on a solar cell and the collector depends on the location of that point [1–4]. And since electron–hole pairs are generated throughout the solar cell, the concept of R_s as a lumped effective series resistance is a simplification. Nevertheless, it is a useful concept to approximate the ohmic losses in a solar cell and for this reason it is important that R_s can be experimentally determined.

Over the years, many different ways of determining the series resistance of a solar cell have been proposed and several studies have compared a selection of different methods for their ability to determine the series resistance of silicon cells [5–10]. To our knowledge no such study exists for III–V concentrator cells. For this reason we have compared the performance of the R_s-determination methods presented in Table 1 using a 20 mm^2 GaAs cell designed to operate at a concentration ratio of 500.

In order to obtain R_s with sufficient accuracy, the *IV*-curve (s) from which R_s is to be derived should be measured at a sufficiently stable high irradiance level, since the series resistance effects only clearly manifest themselves at high currents, as illustrated in Fig. 1. It is not straightforward to achieve high concentration ratios with continuous xenon light sources, and they have the drawback of a significant temporal instability. Xenon flash systems on the other hand can easily reach high concentration ratios, but only for an interval in the order of milliseconds. In addition, the concentration ratio and cell temperature change significantly during this interval, and attempts at extracting *IV*-curves with the required accuracy proved unsuccessful. Since the illumination's spectrum has no influence on the characteristics of a single junction cell's *IV*-curve, we opted to illuminate the solar cell using a purpose built laser based light source, capable of producing very high concentration ratios with negligible temporal instability.

One important aspect to consider is that the actual R_s value of the solar cell is not known. And since there is no guarantee that the mean or median of the R_s values determined by the different methods evaluated in this study lies close to the actual R_s value, it is problematic to establish which of the methods performs best in determining a value for R_s. Therefore, three extra tests were introduced:

1. The R_s values were determined for five different concentration ratios, ranging from 100 to 500. Considering the fact that series resistance effects increase with concentration ratio, which should increase the accuracy with which R_s can be determined, the obtained series resistance values should converge to the relevant R_s value with increasing concentration ratio.
2. The R_s values were not only obtained for the cell as such, but also with an accurately known additional resistance R_a, externally connected in series with the cell. The difference between the two determined R_s values should equal R_a, and the accuracy with which a determination method predicts this value is a measure of its quality. This test is performed using a low ($R_{a,low}$) and a high ($R_{a,high}$) additional series resistance.
3. Each *IV*-curve was measured three times, giving three determined R_s values per determination method for each situation. Three times the standard deviation (3σ) of these values is an indication of the precision of the determination method.

2. Theory

As mentioned before, numerous methods to determine R_s have been published over the years. In a previous study [11] we demonstrated that many of them are more alike than they appear at first sight, and can be arranged in a two-dimensional array. The position of each method in this array is determined by which combination of f, f' and F is used to obtain an expression for R_s, where f stands for the single-diode equation, f' for its derivative with respect to the current and F for its integral over the interval $[0, I_{sc}]$, with I_{sc} the short circuit current. The single-diode equation is given as

$$I = I_L - I_0\left[\exp\left(\frac{V+IR_s}{nV_t}\right)-1\right], \tag{1}$$

where I is the current, I_L is the light induced current, I_0 is the saturation current, n is the diode ideality factor and V is the voltage. Lastly, V_t is the thermal voltage defined as kT_c/q, with k the Boltzmann constant, T_c the absolute temperature of the solar cell and q the elemental charge. Generally I_L or I_L+I_0 is approximated by I_{sc}, I_0 is replaced by $I_c/\exp(V_{oc}/nV_t)$, with V_{oc} the open-circuit voltage, and, where required, $dV/dI|_{MPP}$ is replaced by $-V_{mp}/I_{mp}$, with V_{mp} and I_{mp} the voltage and current at the maximum power point (MPP) respectively. Furthermore, as one is interested in R_s under the most relevant operating conditions, V_{mp} and I_{mp} are taken for V and I. As detailed in Ref. [11], some methods apply elegant procedures to improve the result. In particular the methods of Wolf & Rauschenbach, Swanson and Aberle et al., all based on the *ff* approach, have applied an additional constraint which makes them valid for a much more general equation for a solar cell with a lumped effective series resistance. This equation is given as

$$I = I_L - \sum_{\alpha=a,b,c,\ldots}\left(I_{0,\alpha}\left[\exp\left(\frac{V+IR_s}{n_\alpha V_t}\right)-1\right]\right)-\frac{V+IR_s}{R_{sh}}, \tag{2}$$

280 nm	cap	*n*++ GaAs
30 nm	window	*n* AlInP
150 nm	emitter	*n* GaAs
1800 nm	base	*p* GaAs
40 nm	BSF	*p* $Al_{0.2}Ga_{0.8}As$
300 nm	buffer	*p* GaAs
350 μm	substrate	*p* GaAs

Fig. 2. Layer structure of the GaAs solar cell.

where R_{sh} is the shunt resistance and $I_{0,\alpha}$ and n_α are the saturation current and ideality factor of diode α [12]. Using the approximations $\alpha = 1$ and $R_{sh} \to \infty$ the single-diode equation is obtained. An overview of the methods reviewed in the present work and their expressions for R_s is presented in Table 1. Note that the *ff*, $f'f'$ and *FF* approaches require (a minimum) of two *IV*-curves to be measured. For the general *f*-method a least squares fit is applied to the eleven datapoints surrounding the MPP, in order to avoid the unknown *n*. I_c and V_{oc} are taken as known parameters. This converts the original associated Eq. (4) to

$$R_s = \frac{\sum I_i V_i \sum \lambda_i^2 - V_{oc} \sum I_i \sum \lambda_i^2 - \sum \lambda_i V_i \sum \lambda_i I_i + V_{oc} \sum \lambda_i \sum \lambda_i I_i}{(\sum \lambda_i I_i)^2 - \sum I_i^2 \sum \lambda_i^2}, \quad (3)$$

with $\lambda_i \equiv \ln((I_c - I_i)/I_c)$. A similar procedure for the general f'−method results in the method previously published by Warashina and Ushirokawa [11], so the general f'−method is not discussed separately.

3. Experimental

The solar cell structure was grown by low-pressure MOCVD on a 2 in. GaAs wafer with a (100) 2° off to [110] orientation. Arsine and phosphine were used as group-V source gases, trimethylgallium, trimethyl-indium and trimethyl-aluminium as group-III precursors. For *n*- and *p*-type doping disilane and diethylzinc were used, respectively. The growth took place at temperatures between 600 and 700 °C and at a pressure of 20 mbar. The layer structure is shown in Fig. 2.

Contacts were applied using e-beam evaporation, with the front contact having a square grid with a coverage of 25%, suited for high irradiance levels. The individual cells have an area of 4.9×4.1 mm^2 as defined by a mesa etch. The cell utilised for the present study was covered by a glued glass sheet to avoid accidental damage of the cell and its wiring during examination.

ReRa's Tracer2 software was used to obtain *IV*-curves for a range of concentration ratios provided by a purpose built laser based light source, consisting of 24×1 W, 445 nm laser diodes. Since virtually all the emitted light is focussed onto the solar cell, concentration ratios[1] ranging from 0 up to 550 are achievable for a 4.9×4.1 mm^2 GaAs solar cell. The temporal stability of the illumination is excellent, with a long term instability of only 0.04%, as is the spatial non-uniformity of $< 2\%$ over the whole range of concentration ratios. A detailed description of this illumination set-up will be published elsewhere [20]. For each *IV*-curve measured at a concentration ratio of interest at least two additional *IV*-curves were obtained with accurately known additional resistors ($R_{a,low} = 4.40 \pm 0.04$ mΩ and $R_{a,high} = 51.67 \pm 0.04$ mΩ) connected in series to the solar cell.

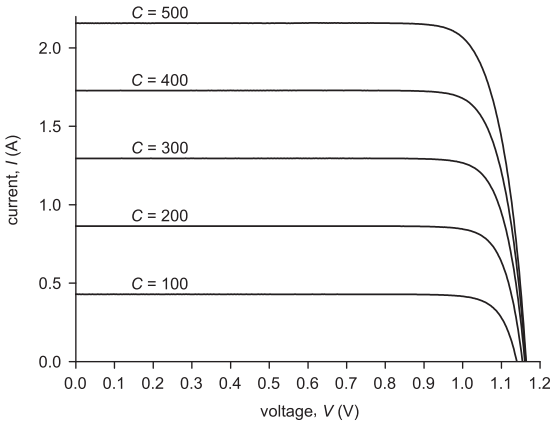

Fig. 3. Raw data *IV*-curves obtained at various concentration ratios.

All measurements were performed in triplicate and each *IV*-curve consisted of 501 datapoints measured over the −0.1–1.3 V interval (−0.1–1.4 V for the dark curves). All measurements were performed at a sensor temperature T_s of 25 °C unless mentioned otherwise. The temperature sensor was connected next to the cell on its aluminium carrier, with T_s kept constant utilising a PID controlled Peltier element under the carrier. Temporal monitoring of T_s revealed that it did not vary more than 0.02 °C under stable conditions. During the measurement of an *IV*-curve, a small dip of at most 0.15 °C would appear, resulting from the fact that the solar cell can release a varying fraction of the incoming power as electric power during this period.

Despite these considerable efforts to keep the cell temperature T_c constant, it still increases with concentration ratio as a result of the measurement configuration. Because with virtually all the light focussed onto the solar cell, the cell temperature must exceed the temperature of the sensor connected next to the cell on the same aluminium carrier, with the difference being proportional to the concentration ratio, as detailed in the Appendix. To determine the proportionality factor, as well as each method's sensitivity to the increase of the cell temperature with concentration ratio, a series of $C = 500$ and 550 *IV*-curves[2] was measured for T_s ranging from 25 to 29 °C. An indicative IR temperature measurement revealed that the cell was not significantly heated compared to the carrier at $C = 500$.

4. Results and discussion

The *IV*-curves measured when no additional resistance was connected in series to the cell, at concentration ratios of 100, 200, 300, 400 and 500 are displayed in Fig. 3. Note the smoothness of the raw data curves in comparison with typical *IV*-curves obtained from concentrator cells under a continuous high flux xenon light source [21] or a flash sun simulator [22].

The series resistance values obtained from the *IV*-curves by the different R_s-determination methods are displayed in Fig. 4a as a function of concentration ratio. In addition, the 3σ values of the determined R_s values and the deviations from the additional resistances $R_{a,low}$ and $R_{a,high}$ are plotted for the same range of concentration ratios in Fig. 4b, c and d respectively. Note that the curve of Jia et al. does not appear in Fig. 4d since it is continuously below the plotted range. Likewise, the method of Warashina & Ushirokawa ($f'-$) and the general method of approach $f'f'$ fall

[1] The concentration ratio was defined as the ratio between the solar cell's I_{sc} value under concentration and its I_{sc} value measured under the AM1.5G spectrum at an irradiance of 1000 W m^{-2}.

[2] Any associated lower concentration ratio *IV*-curve was measured with $T_s = 25$ °C.

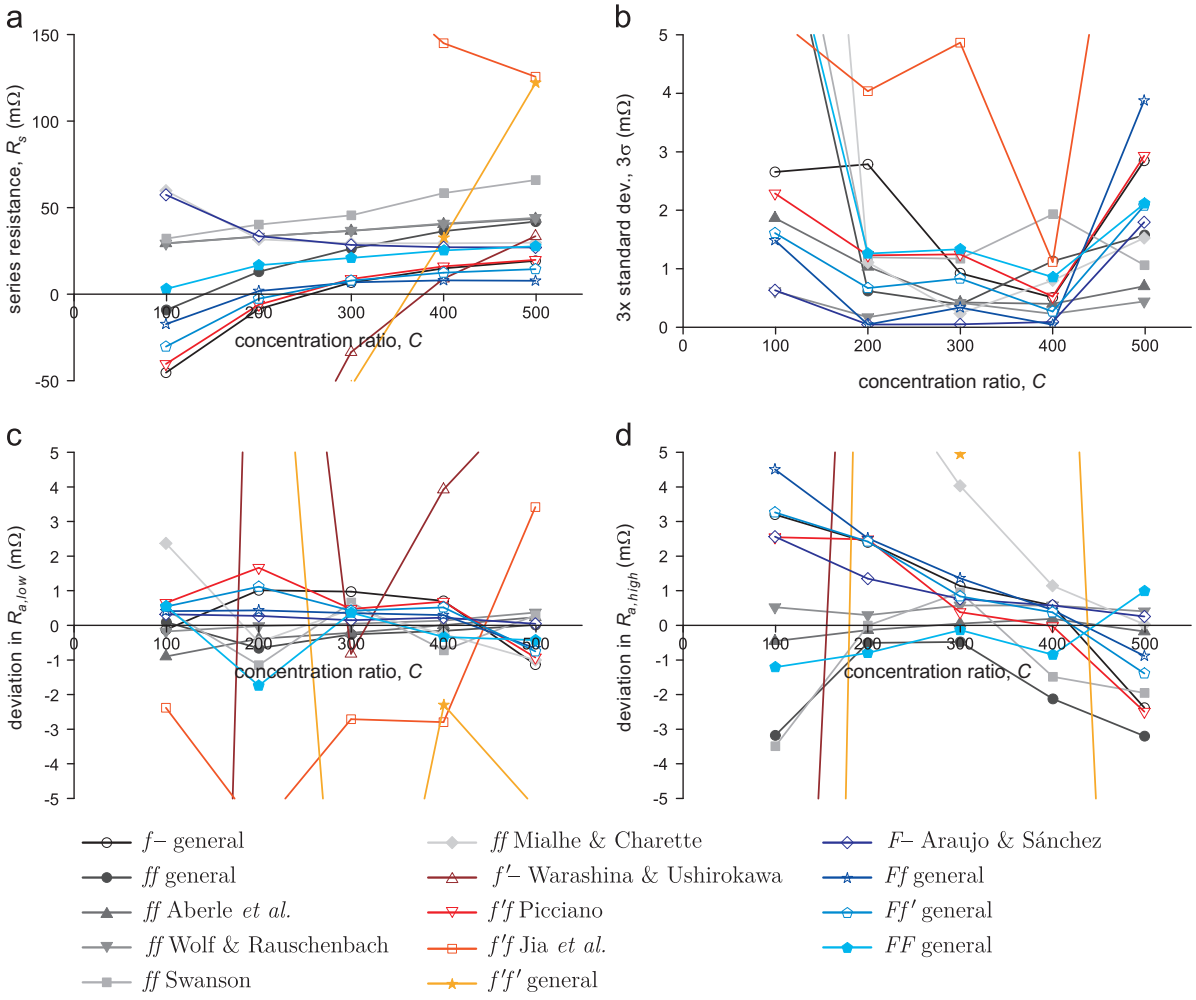

Fig. 4. Performance of the tested R_s-determination methods as a function of concentration ratio. Plotted are (a) the determined series resistance of the GaAs solar cell, (b) 3σ of the determined R_s value, (c) the deviation from the additional resistance $R_{a,low} = 4.40 \pm 0.04$ mΩ and (d) the deviation from the additional resistance $R_{a,high} = 51.67 \pm 0.04$ mΩ.

outside the plotted range of Fig. 4b. It is no surprise that these three methods are precisely the ones which show the most erratic behaviour in Fig. 4a. Although these three methods all lie in category f', it is not their use of the relation $dV/dI|_{MPP} = -V_{mp}/I_{mp}$ that causes the erratic behaviour, since the method of Picciano and the general method of approach Ff' also use it and behave much less erratic. Neither is the condition that $n=1$ at V_{oc}, while n at the MPP is not set to a specific value, as applied by the method of Jia et al., the cause for this method's erratic behaviour. Because, as we discussed in Ref. [11], this condition can also be applied to other methods, for example the general *ff* method, and this resulted in an $R_s(C)$ curve (not shown) that virtually overlaps the curve of the general *ff* method without this condition applied. Instead, the erratic behaviour of the $R_s(C)$ curve of the method of Jia et al. must be caused by its implicit assumption $dn/dI|_{MPP} \approx 0$ being incorrect [11]. The behaviour of the curves produced using the method of Warashina & Ushirokawa ($f'-$) can be attributed to the fact that the linear fit of dV/dI as a function of $-1/(I_{sc}-I)$ requires such a long extrapolation to determine R_s and that its determined R_s value is very sensitive to the current at which it is obtained, as discussed in Ref. [11]. As for the general $f'f'$ method, it turns out that the difference between the two terms in the numerator of Eq. (16) is very small. This causes small measurement errors to have a large effect on the value of R_s determined by this method.

Although the method of Picciano ($f'f$) and the general methods of *f*–, *ff*, *Ff* and Ff' are not all from the same category and do not all use either a single or a pair of *IV*-curves, their $R_s(C)$ curves do follow a similar trend: initially R_s increases strongly with C and then stabilises at high C. What is very important to note is that all these methods present a *negative* series resistance at low C. Even though their determined R_s values are obviously incorrect at low C, they do determine accurate values for the additional series resistances $R_{a,low}$ and $R_{a,high}$. This suggests that although these methods are not suitable for absolute R_s measurements, they are suitable for relative R_s measurements, for instance to experimentally compare various contact grid configurations.

An overview of the performance of the R_s-determination methods for the four applied tests is presented in Table 2. The values presented for each method are the root mean squares of the corresponding datapoints from Fig. 4b, c and d. Deviations larger than 1 mΩ are considered questionable and are indicated with an orange background, while deviations larger than 5 mΩ are considered inadequate and are indicated with a red background. Other values have a green background and are considered satisfactory. A similar color coding is used for each method's $R_s(C)$ characteristic. This overview shows that there is only a select group of methods which do not have at least one 'inadequate' indication. Apart from the three methods from approach *ff* that satisfy the more general diode equation (Swanson, Wolf & Rauschenbach and Aberle et al.) these are the method of Araujo & Sánchez (*F*-) and the general *FF* method. A more detailed plot of $R_s(C)$ for this select group of methods is presented in Fig. 5.

Table 1
Two-dimensional array arrangement of expressions[a] for a solar cell's lumped effective series resistance R_s, resulting from the single-diode equation (f), its derivative (f'), its integral (F) and combinations thereof. The expressions for the methods of Wolf & Rauschenbach, Swanson and Aberle et al. are also valid for the more general equation (2).

	Category		
	f	***f′***	***F***
2nd index			
–	*f*-general: $\frac{nV_t\lambda+V_{oc}-V}{I}$ (4)	*f′*−general: $\frac{V_{mp}}{I_{mp}}-\frac{nV_t}{I_a}$ (5)	*F*-general=Araujo & Sánchez [14]: $\frac{2}{I_b}\left(\frac{V_{oc}I_c-A}{I_{sc}}-nV_t\right)$ (7)
		Warashina & Ushirokawa [13]: $\frac{\sum\xi_i\sum\xi_iV_i'-\sum\xi_i^2\sum V_i'}{N\sum\xi_i^2-(\sum\xi_i)^2}$ (6)	
f	*ff* general: $\frac{(V_{oc1}-V_1)\lambda_2-(V_{oc2}-V_2)\lambda_1}{I_1\lambda_2-I_2\lambda_1}$ (8)	*f′f* general=Picciano [18]: $\frac{I_a\lambda\frac{V_{mp}}{I_{mp}}+V_{oc}-V}{I+I_a\lambda}$ (13)	*Ff* general: $\frac{2\lambda}{I_b\lambda+2I}\left(\frac{V_{oc}-V}{\lambda}+\frac{V_{oc}I_c-A}{I_{sc}}\right)$ (15)
	Aberle et al. [7]: $\frac{(V_2-V_1)}{I_1}$ (9)	Jia et al. [19]: $\frac{V_{mp}(I_d-I_{mp})}{I_{mp}(I_d+I_{mp})}$ (14)	
	Wolf & Rauschenbach [15]: $\frac{(V_{oc2}-V_1)}{I_1}$ (10)		
	Swanson [16]: $\frac{(V_2-V_1)}{I_{L1}-I_{L2}}$ (11)		
	Mialhe & Charette [17]: $\frac{(V_{oc2}-V_{mp2}-I_{mp2}R_a)\lambda_{mp1}}{I_{mp2}\lambda_{mp1}-I_{mp1}\lambda_{mp2}}-\frac{(V_{oc1}-V_{mp1})\lambda_{mp2}}{I_{mp2}\lambda_{mp1}-I_{mp1}\lambda_{mp2}}$ (12)		
f′	see *f′f*	*f′f′* general: $\frac{I_{a1}\frac{V_{mp1}}{I_{mp1}}-I_{a2}\frac{V_{mp2}}{I_{mp2}}}{I_{a1}-I_{a2}}$ (16)	*Ff′* general: $\frac{2}{I_{sc}-2I_{mp}}\left(\frac{V_{mp}I_a}{I_{mp}}-\frac{V_{oc}I_c-A}{I_{sc}}\right)$ (17)
F	see *Ff*	see *Ff′*	*FF* general: $\frac{2}{I_{b1}-I_{b2}}\left(\frac{V_{oc1}I_{c1}-A_1}{I_{sc1}}-\frac{V_{oc2}I_{c2}-A_2}{I_{sc2}}\right)$ (18)

R_a is a known additional resistance, externally connected in series to the cell for the second *IV*-curve.
For the methods of Wolf & Rauschenbach, Swanson and Aberle et al. there is a dependency between the variables with subscripts 1 and 2, in the form of $I_{L1}-I_1=I_{L2}-I_2$.

[a] Where: A is the area underneath the *IV*-curve in the first quadrant; N is the number of datapoints used; $I_c\equiv I_L+I_0$; $\lambda\equiv\ln((I_c-I)/I_c)$; $\lambda_{mp}\equiv\ln((I_c-I_{mp})/I_c)$; $\lambda_i\equiv\ln((I_c-I_i)/I_c)$; $\xi_i\equiv-(I_c-I_i)^{-1}$; $V_i'\equiv dV/dI|_i$; $I_a\equiv I_c-I_{mp}$; $I_b\equiv 2I_c-I_{sc}$; $I_d\equiv(\lambda_{mp}+V_{oc}/V_t)I_a$.

Note that the plot from the method of Mialhe & Charette is included as well, even though its root mean squares of 3σ and of the deviation from $R_{a,high}$ are >5 mΩ, due to large values at low C. From Fig. 5 it is clear that there is still a significant spread between the curves of (most of) these methods. In addition, for each individual method the determined values for R_s vary with C. General explanations for this behaviour are discussed first, followed by separate discussions on each of these six methods.

4.1. Variation of R_s with C

According to a study by Araujo et al. [23] the variation of R_s with C might be caused by the fact that the series resistance effects are modelled by a constant lumped effective series resistance. In their paper they discuss the simplified case of a (unit) solar cell of length L and width S with a single contact grid finger along one of the sides of length L. Base and emitter resistivities and thicknesses are ρ_b, ρ_e, t_b and t_e respectively, and grid and contact resistances are ignored. The base and emitter resistances are given by $R_b\equiv\rho_b t_b/LS$ and $R_e\equiv\rho_e S/Lt_e$ respectively, and it is shown that as long as current crowding phenomena are small, which is the case when $R_b/R_e\gg 1$ and/or $IR_s\lesssim nV_t$, the series resistance effects can be well modelled by a lumped effective series resistance equalling $R_s=R_b+R_e/3$. However, when current crowding phenomena do become important, the series resistance actually starts to vary with both C and I: for dark *IV*-curves R_s decreases from $R_b+R_e/3$ at low magnitude currents to $\sqrt{R_eR_b}$ at high magnitude currents. For illuminated curves at low concentration ratios, R_s is stable at $R_b+R_e/3$, but at high concentration ratios R_s decreases from $R_b+R_e/2$ at high currents to $\sqrt{R_eR_b}$ at low currents. The dependence is also illustrated in Fig. 6.

In the present case $R_b/R_e\approx 7\times10^{-3}$ so the first condition is not satisfied. However, the second condition $IR_s\lesssim nV_t$ is satisfied for $C<250\pm70$, depending on the value of the diode ideality factor.[3]

[3] In the single-diode model the value of n varies with current and concentration ratio [11], while the multidiode model is valid for any number of diodes, and

Table 2
Overview of the performance of the R_s-determination methods for the four applied tests. The values presented for each method are the root mean squares of its corresponding datapoints from Fig. 4b, c and d. The background colour of a cell indicates whether the contents is satisfactory (green), questionable (orange) or inadequate (red).

approach and method	characteristic of $R_s(C)$ curve	root mean square of deviation in $R_{a,low}$ (mΩ) ■ > 5.0, ■ > 1.0, ■ ≤1.0	root mean square of deviation in $R_{a,high}$ (mΩ) ■ > 5.0, ■ > 1.0, ■ ≤1.0	precision: root mean square of 3σ (mΩ) ■ > 5.0, ■ > 1.0, ■ ≤1.0
f– general	< 0 at low C	0.9	2.2	2.2
ff general	< 0 at low C	0.3	2.3	3.6
ff Aberle *et al.*	increases linearly with C	0.5	0.2	1.0
ff Wolf & Rauschenbach	increases linearly with C	0.2	0.5	0.4
ff Swanson	increases linearly with C	0.7	2.0	4.2
ff Mialhe & Charette	unstable at low C	1.2	20.7	8.8
f′– Warashina & Ushirokawa	< 0 for most of the range	33.8	20.5	98.1
f′f Picciano	< 0 at low C	1.0	2.0	1.9
f′f Jia *et al.*	very unstable	3.7	15.6	6.1
f′f′ general	< 0 for most of the range	19.4	51.1	276.4
F– Araujo & Sánchez	unstable at low C	0.2	1.4	0.9
Ff general	< 0 at low C	0.4	2.4	1.9
Ff′ general	< 0 at low C	0.7	2.0	1.3
FF general	unstable at low C	0.9	0.9	3.7

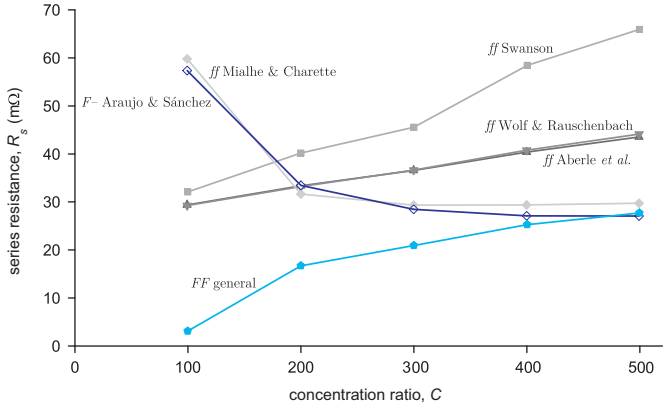

Fig. 5. Series resistance as a function of concentration ratio, for a selected number of R_s-determination methods. Note that the curves of the method of Wolf & Rauschenbach and that of Aberle et al. virtually overlap.

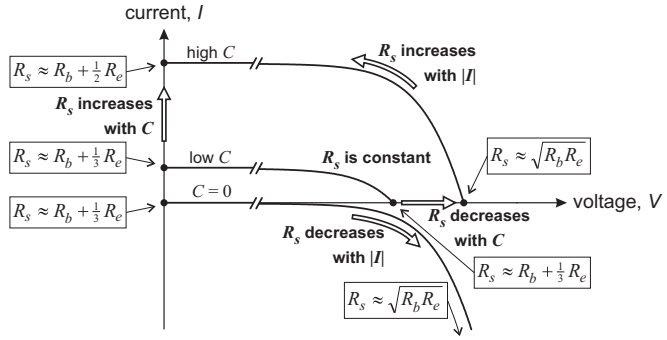

Fig. 6. Variation of R_s with current and concentration ratio for both dark and illuminated conditions, according to the theory by Araujo et al. [23].

Whether R_s should increase or decrease with increasing C is not clear, since the maximum power point lies in between I_{sc} (where R_s increases with C) and V_{oc} (where R_s decreases with C). However, none of the curves in Fig. 5 start to rise or drop at $C > 250 \pm 70$. On the contrary, the curves of the methods of Araujo & Sánchez, Mialhe & Charette and *FF* general all tend to stabilise at high C, and the curves of the methods of Aberle et al., Wolf & Rauschenbach and Swanson all display a (virtually) linear increase with C over the entire measured range.

This means that the theory of Araujo et al. does not explain the observed effects. Instead, the stabilisation at high C of the $R_s(C)$ curves of the methods of Araujo & Sánchez, Mialhe & Charette and *FF* general is more likely due to the fact that the accuracy with which R_s can be determined increases with C, as mentioned in the introduction. A plausible explanation for the linear increase of R_s with C for the methods of Aberle et al., Wolf & Rauschenbach and Swanson is the temperature effect discussed below.

4.1.1. *Temperature effect*

As discussed in Section 3, the cell temperature T_c increases with concentration ratio, even if the sensor temperature T_s is kept constant. In fact, as discussed in the Appendix, the increase in cell temperature from the intended 25 °C can be expressed as

$$\Delta T_c = \Delta T_s + gC, \tag{19}$$

(*footnote continued*)
does not predict a single value for n. However, we can safely assume that n will have a value between 1 and 2. And since R_s was determined for MPP conditions, I equals I_{mp}.

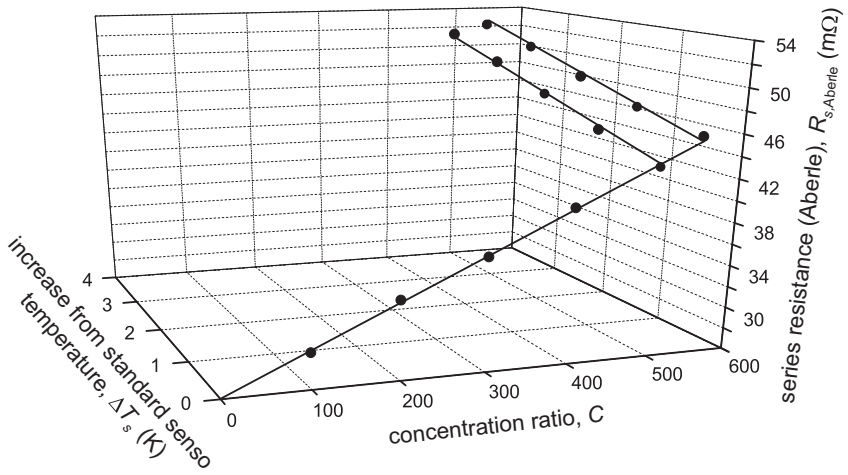

Fig. 7. R_s determined using the method of Aberle et al. as a function of C and ΔT_s. Also displayed is the least squared fit to $R_{s,\mathrm{Aberle}} = a + bC + \beta\Delta T_s$. Note that the sensor temperature was only varied for the illuminated curves and kept at 25 °C for the dark curve.

with g a constant and $\Delta T_s \equiv T_s - 25$ K. And although the effect of ΔT_c on the *actual* R_s value will be negligible for the considered temperature range, the *determined* values of R_s do strongly depend on ΔT_c for some of the methods. This follows from R_s values determined using $C = 500$ and 550 *IV*-curves[4] measured with ΔT_s set at 0–4 K, which show a linear increase with ΔT_s (and, therefore, ΔT_c according to Eq. (19)) for the methods of Wolf & Rauschenbach, Aberle et al. and Swanson. The rates of increase of the first two are similar, while the latter has a higher rate, which agrees with the behaviour shown in Fig. 5. The methods of Araujo & Sánchez, Mialhe & Charette and *FF* general also show a linear relation, albeit with (much) lower rates. The $R_s(\Delta T_s)$ data from the method of Aberle et al. is displayed in Fig. 7, together with the $R_s(C)$ datapoints of the method of Aberle et al. from Fig. 5.

Since the ΔT_c value associated with the required dark curve is known to be zero (because under those conditions $\Delta T_c = \Delta T_s$ according to Eq. (19)), the data in Fig. 7 is well suited to deduce the actual cell temperature under illumination. From the figure it follows that the data can be well fitted using

$$R_{s,\mathrm{Aberle}} = a + bC + \beta\Delta T_s, \tag{20}$$

with $a = 26.1 \pm 0.3$ mΩ, $b = (3.55 \pm 0.07) \times 10^{-2}$ mΩ and $\beta = 1.78 \pm 0.06$ mΩ/K according to a least squares fit. Note that $R_{s,\mathrm{Aberle}}$ is used here to clearly indicate that the equation applies to the R_s value *as determined* by the method of Aberle et al., and not the *actual* R_s value.

Substituting ΔT_s from Eq. (19) into Eq. (20) yields

$$R_{s,\mathrm{Aberle}} = a + (b - \beta g)C + \beta\Delta T_c. \tag{21}$$

Assuming that $R_{s,\mathrm{Aberle}}$ is only indirectly dependent on C (through ΔT_c being a function of C), $b - \beta g$ must equal zero, so $g = b/\beta = (2.00 \pm 0.08) \times 10^{-2}$ K. According to Eq. (19) this means that with $\Delta T_s = 0$ K at $C = 500$, $\Delta T_c = 10.0 \pm 0.4$ K, i.e. the cell temperature T_c equalled 35.0 ± 0.4 °C. This is in agreement with the indicative IR temperature measurement which indicated that at $C = 500$ the cell was not significantly heated compared to the carrier.

[4] Any associated lower concentration ratio *IV*-curves were measured with $T_s = 25$ °C.

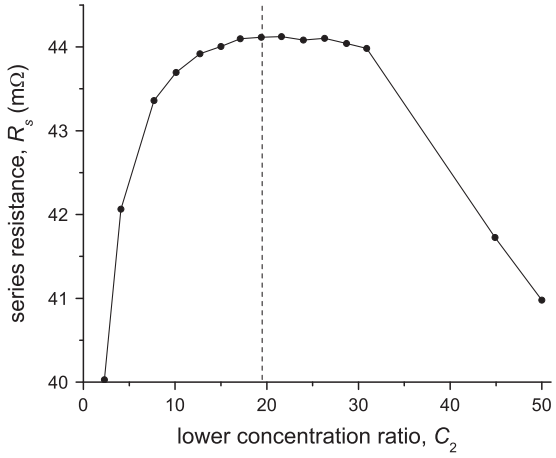

Fig. 8. Plot of R_s for $C_1 = 500$, determined using the method of Wolf & Rauschenbach, for a range of lower concentration ratios C_2. The dashed line indicates $C_2 = 19.5$, the value at which $I_{sc2} = I_{sc1} - I_{mp1}$.

4.2. Method of Aberle et al.

This method is one of the three R_s-determination methods which is valid for the more general diode equation, given by Eq. (2). It requires the measurement of an *IV*-curve at the concentration ratio of interest and one in dark conditions. Strictly speaking, expression (9) for R_s should read [11]:

$$R_{s1} = \frac{V_2 - V_1}{I_1} - \frac{(I_{L1} - I_1)R_{s2}}{I_1}, \tag{22}$$

with $R_{s\ 1}$ and $R_{s\ 2}$ the series resistance in illuminated and dark conditions, respectively.[5] However, Aberle et al. assume the second term on the right-hand side of the equation is negligible. This assumption is validated by the fact that if this term *is* included,[6] R_s ($= R_{s1}$) is only reduced by about 1 mΩ over the entire C range. In addition, together with the method of Wolf & Rauschenbach, this method determines the values of $R_{a,low}$ and $R_{a,high}$ with the highest accuracy, as can be seen in Table 2. The precision of this method is also good, since its 3σ values are quite low.

[5] Due to a different current flow pattern under these conditions, $R_{s2} < R_{s1}$ [7].

[6] With $R_{s\ 2}$ taken as $(V_R - V_{oc1})/I_{L1}$, where V_R is the voltage of the dark curve for which the current equals $-I_{L1}$ [11].

The method of Aberle et al. is quite sensitive to the increase in cell temperature with C, with its determined R_s values increasing with 3.53×10^{-2} mΩ per unit increase in C. Judging from Fig. 4b and the fact that its $R_s(C)$ curve is linear over the entire C range, it seems that this method does not suffer from a lower accuracy at the lower end of the studied C range. This means that with the present dataset the best value for R_s that can be obtained using this method would be the extrapolation to $C=0$, where the cell temperature would equal 25 °C. This results in $R_s = 26.0 \pm 0.3$ mΩ.

4.3. Method of Wolf & Rauschenbach

As with the method of Aberle et al. this method is valid for the more general diode equation and requires the measurement of two *IV*-curves with the first one at the concentration ratio of interest C_1. The second one should not be measured in the dark but at a relatively low concentration ratio C_2, at which $I_{sc2} = I_{sc1} - I_{mp1}$. The accuracy with which the lower concentration ratio C_2 can be set determines how far the point at which R_s is determined deviates from the MPP, which in turn could influence the value of R_s. This turns out to be a minor influence, as illustrated in Fig. 8, where R_s is displayed for $C_1 = 500$, determined for a range of C_2 values. It is clear that C_2 can deviate quite substantially from its intended value of 19.5 before R_s digresses more than 1 mΩ. The fact that the accuracy required for the C_2 setting is easily met is also indicated by the fact that this method, together with the method of Aberle et al., has the best precision and the best accuracy with which it produces the values of the known additional external resistors $R_{a,low}$ and $R_{a,high}$. This good performance is not surprising, since in our previous study this method was found to be the most solid in theory [11].

As can be seen in Fig. 5, the $R_s(C)$ curve of the method of Wolf & Rauschenbach virtually overlaps with that of the method of Aberle et al. This means that this method's sensitivity to the increase of cell temperature with concentration ratio is very close to that of the method of Aberle et al. discussed previously. Extrapolating this method's $R_s(C)$ curve to $C=0$ results in $R_s = 25.6 \pm 0.3$ mΩ as the best value for R_s that can be obtained using the method of Wolf & Rauschenbach. It differs only 0.4 mΩ from the best value according to the method of Aberle et al.

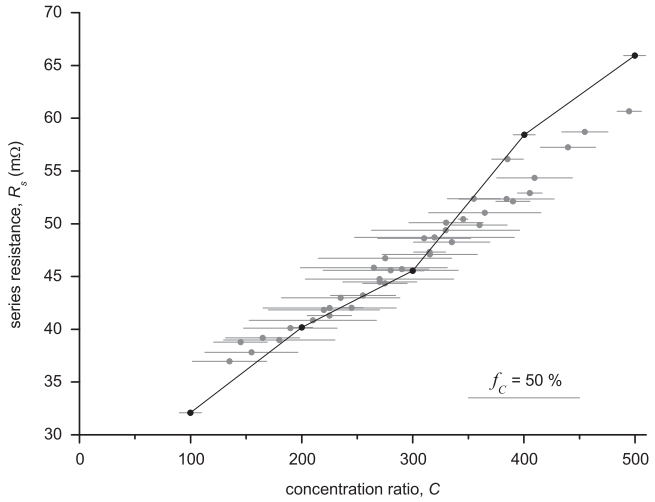

Fig. 9. Method of Swanson's dependence on f_C. The markers indicate the series resistance as a function of concentration ratio, and the horizontal lines indicate the magnitude of f_C for each datapoint (note the horizontal scale bar indicating 50%). Note that one datapoint at $C=445$ falls outside the plotted range, with $R_s=7.9$ mΩ. Its irregular value is due to the very low value of the associated f_C of 1.1%, i.e. the two curves have a minimal difference in concentration ratio, resulting in a high error. The connected black markers (with $f_C=10\%$) are the actual datapoints used for the evaluation of the method of Swanson.

4.4. Method of Swanson

Like the methods of Aberle et al. and Wolf & Rauschenbach, this method is valid for the more general diode equation and also requires the measurement of two curves. In this case, one curve should be measured at a concentration ratio C_1 slightly above the concentration ratio of interest C, and one slightly below it, at C_2. The respective curves were measured at $C_1 = 1.1C$ and $C_2 = 0.9C$ for each value of C, i.e. $f_C \equiv (C_1 - C_2)/(C_1 + C_2) \times 100\% = 10\%$. To give an impression of the sensitivity of this method to the value of f_C, $R_s(C)$ is displayed in Fig. 9 for all the possible combinations of the measurements performed for the method of Swanson, with their associated f_C values, ranging from 1.1 to 71.9%, indicated. Although there is no clear correlation between R_s and the magnitude of f_C, the spread in R_s values is quite substantial at high concentration ratios. This means that the (arbitrary) choice of f_C has a large influence on the R_s value determined utilising the method of Swanson. Also note that the R_s values with $f_C=10\%$ lie at the low end of the range at low C and at the high end of the range at high C. Still, irrespective of the choice of f_C, the R_s value determined by the method of Swanson increases strongly with C.

The value of R_s should ideally be determined at the MPP of the *IV*-curve obtained at the concentration ratio of interest. Since the two curves required for this method are, however, obtained at $1.1C$ and $0.9C$, V_{av} is taken as the average of the maximum power point voltages of both curves. For $C=500$, V_{av} only deviates 0.9 mV from the V_{mp} value of the *IV*-curve actually obtained at $C=500$. This small deviation has negligible influence on the obtained value of R_s, since the dependence of R_s on $\Delta V \equiv V_{av} - V_{mp}$ was found to be linear for $|\Delta V| < 20$ mV, with $R_s = -0.123\Delta V + 65.7$ mΩ (with ΔV in mV). This means that in this case the deviation in R_s only amounts to 0.1 mΩ.

As can be seen in Fig. 5, the method of Swanson is much more sensitive to the increase in cell temperature with C as the methods of Aberle et al. and Wolf & Rauschenbach, with its determined R_s values increasing approximately linear with 8.60×10^{-2} mΩ per unit increase in C. This is not surprising, since the difference between the two voltages in the numerator of Eq. (11) is only small, so that temperature induced changes in these voltages have a relatively strong effect.

Another factor causing this method to yield such high values of R_s is the fact that this method assumes R_s to be constant, even though R_s increases with C (due to the increase in cell temperature). With $R_{s\,1}$ and $R_{s\,2}$ the actual series resistances at C_1 and C_2, the full expression for $R_{s\,1}$ is [11]

$$R_{s1} = \frac{V_2 - V_1}{I_{L1} - I_{L2}} - \frac{I_2}{I_{L1} - I_{L2}} \Delta R_s, \tag{23}$$

with $\Delta R_s \equiv R_{s1} - R_{s2}$. Since the method of Swanson assumes $R_{s1} = R_{s2} = R_s$, i.e. $\Delta R_s = 0$, it ignores the second term and, therefore, determines a higher value for R_s.

Apart from the small dip at $C=300$, this method's $R_s(C)$ curve is linear over the entire C range. Like the methods of Aberle et al. and Wolf & Rauschenbach, this method does not seem to suffer from a lower accuracy at the lower end of the studied C range either. Extrapolating the $R_s(C)$ curve to $C=0$ results in $R_s = 23 \pm 3$ mΩ as the best value for R_s that can be obtained using the method of Swanson.

4.5. Method of Araujo & Sánchez

The $R_s(C)$ curve of this method follows a completely different trend than those of the three previously discussed methods. Instead of a linear increase from low to high C, R_s displays an exponential-like decrease, and converges to ~27 mΩ at high C. Contrary to the other three methods, the R_s value produced by this

method is not strongly affected by temperature, at only 0.26 mΩ/K at $C=500$. With an expected $\Delta T_c = 10$ K at $C=500$, this would suggest that the determined value of R_s is only 2.6 mΩ too high. Instead, the strong initial decrease in R_s is presumably caused by the fact that the diode ideality factor n is taken as 1 by this method, even though its actual value at low C will be >1 for a large portion of the *IV*-curve [11]. At higher concentration ratios, n will converge to 1 because then the emitter diffusion current is dominant along almost the entire *IV*-characteristic. This causes the R_s value determined by this method to approach the actual R_s value of the cell at reasonably high C values only. However, one should keep in mind that at even higher C, Auger recombination can start to play a role [24]. Since Auger recombination is associated with $n = 2/3$, this will again introduce a deviation in the R_s values predicted by this method for very high concentration ratios. Compared to the other five selected methods, this method does have the practical advantage that it only requires a single *IV*-measurement. Considering the stabilisation of R_s at high C and taking the small temperature effect into account, the best value for R_s that can be obtained with the method of Araujo & Sánchez is 24 ± 2 mΩ.

4.6. Method of Mialhe & Charette

What makes this method stand out from other methods requiring the measurement of two *IV*-curves is that in this case the two curves are not measured at different concentration ratios. Instead, a known additional resistance R_a is externally connected in series to the cell for the second *IV*-curve. This way, there will only be a small difference between $I_{mp\,1}$ and $I_{mp\,2}$, so that the diode ideality factor n (which, although mostly ignored, is a function of I and C for the single-diode model [6]) will not vary much between them [11]. The value for the additional resistance used in the present study was 183.16 ± 0.06 mΩ.

As illustrated by Fig. 5, the $R_s(C)$ curve of this method shows a similar trend as the curve from the method of Araujo & Sánchez. In addition, the temperature dependence of its determined R_s values is virtually the same (0.25 mΩ/K at $C=500$). However, these similarities are coincidental because the method of Mialhe & Charette does not assume $n=1$. The fact that R_s determined at low C deviates a lot from the value it diverges to at higher C is instead caused by the tiny difference between $I_{mp\,1}$ and $I_{mp\,2}$ at low C, so that a small measurement error has a large effect on the determined value of R_s, according to Eq. (12). This is substantiated by the fact that the precision is generally good, except at $C=100$ where it is very poor, as illustrated by Fig. 4b. In addition, measurements where the additional resistance $R_{a,high}$ is used as R_a result in an $R_s(C)$ curve (not shown) that is completely different from the displayed curve at low C, but approaches it to within 1 mΩ at high C. This indicates that this method works well, provided that C is sufficiently high. Based on the stabilisation of $R_s(C)$ for sufficiently high C and taking the small temperature effect into account, the best value for R_s that can be obtained using the method of Mialhe & Charette is 27.3 ± 0.5 mΩ.

4.7. General method of approach FF

This method requires one curve to be measured at a concentration ratio C_1 slightly above the concentration ratio of interest C, and one slightly below it, at C_2. As with the method of Swanson, the respective curves were measured at $C_1 = 1.1C$ and $C_2 = 0.9C$ for each value of C.

According to Fig. 4b this method's 3σ value is very high at $C=100$, which is reflected in the divergent R_s value at that concentration ratio compared to the rest of the curve in Fig. 5. It is unclear whether the curve then slowly converges to a stable value at high C, or that is simply keeps increasing with C, or if it displays a combination of both. So unlike the five previously discussed methods, it is not possible to give a best value of R_s obtained with this method.

4.8. Actual R_s value

None of the selected methods is perfect: some are very sensitive to temperature, others do not perform well until C reaches several hundred suns. Still, for all but one of the selected methods it was possible to designate an optimal value for R_s (in mΩ):

Aberle et al.:	26.0±0.3
Wolf & Rauschenbach:	25.6±0.3
Swanson:	23±3
Araujo & Sánchez:	24±2
Mialhe & Charette:	27.3±0.5
Weighted average:	26.0±0.2

As mentioned in the introduction, the problem with determining the accuracy of the methods is that the actual R_s value of the solar cell is unknown. Still, the fact that none of the above values deviates more than 3.0 mΩ from their weighted average of 26.0 mΩ does suggest that the actual R_s value will be (quite) close to this. It also suggests that each of these methods, when applied correctly, will provide a value close to the actual value of R_s.

For the three methods which are valid for the more general diode equation, i.e the methods of Aberle et al., Wolf & Rauschenbach and Swanson, a correct application means that the cell temperature is not allowed to deviate much from its intended value. As long as that is the case these methods will determine a good R_s value for $C \geq 100$ or even lower. The method of Swanson is clearly the least well performing of the three, due to its stronger sensitivity to cell temperature deviations and its lower precision. Such a strict cell temperature control is not required for the methods of Mialhe & Charette and Araujo & Sánchez. Instead, a correct application of these methods requires a sufficiently high concentration ratio ($\gtrsim$300), although C is not allowed to become too high for the method of Araujo & Sánchez.

5. Conclusions

The present study compares fourteen series resistance determination methods, from nine different approaches as categorised by Ref. [11], for their ability to experimentally determine R_s of a III–V concentrator solar cell. Since the actual R_s value of the cell is unknown, three tests were introduced: R_s is determined as a function of concentration ratio, the precision (3σ) is measured and the accuracy in determining an additional resistance, externally connected in series with the cell, is tested.

The study reveals that only methods from the *ff* approach perform adequately. The only exception is the method of Araujo & Sánchez, which is surprising since theoretical considerations suggest that it would perform the worst because it assumes $n=1$. However, at sufficiently high concentration ratios n does approach 1, and it is indeed at high concentration ratios ($\gtrsim$300) that this method performs well. It should be noted, however, that it is expected to become less accurate at even higher C, when Auger recombination starts to play a role.

Not all methods from the *ff* approach perform adequately, though. Only the method of Mialhe & Charette and the methods that are valid for the more general diode equation do. Note that the latter do not assume a single and constant n, while for the former the difference in n values associated with the points from the two curves will be minimum. From this viewpoint one would expect the method of Jia et al. to perform well too, since it also does not assume n to be

constant throughout the *IV*-curve. Its actual performance was very poor, however, which must be caused by the implicitly included assumption $dn/dI|_{MPP} \approx 0$ being incorrect.

But even the methods that perform adequately are not perfect. The R_s values determined by the methods that are valid for the more general diode equation, i.e. the methods of Aberle et al., Wolf & Rauschenbach and Swanson, all increase with C. It was demonstrated that this is most probably caused by an increase in cell temperature with C, despite considerable efforts to keep a constant cell temperature. The method of Swanson is most sensitive to the temperature effect and in addition depends on the (arbitrary) choice of f_C. The methods of Wolf & Rauschenbach and Aberle et al. determine the values of the additional resistances with the highest accuracy and have the best reproducibility. In addition, their $R_s(C)$ curves virtually overlap, even though the method of Wolf & Rauschenbach is the best in theory. The method of Aberle et al. has the practical advantage that it does not require an (accurate) setting of the concentration ratio for the second *IV*-curve. The methods of Araujo & Sánchez and Mialhe & Charette on the other hand are not as sensitive to temperature variations, so if the cell temperature cannot be well controlled then these can be the preferred methods, as long as R_s is measured at sufficiently high concentration ratios. Considering these findings it would be preferable if the International Electrotechnical Commission adopted either the method Wolf & Rauschenbach or that of Aberle et al. as its series resistance determination standard (while keeping its prescribed narrow range in allowed cell temperatures), instead of its current method which is that of Swanson [25].

None of the best R_s values determined using the methods of Wolf & Rauschenbach, Aberle et al., Swanson, Mialhe & Charette and Araujo & Sánchez deviates more than 3.0 mΩ from their weighted average of 26.0 mΩ. So even though the actual R_s value of the solar cell is unknown this suggest that it will be close to this. It also suggests that, as long as they are applied correctly, each of these methods will provide a value quite close to the actual value of R_s. When the actual solar cell can be kept at the appropriate temperature, the three methods which are valid for the more general diode equation are expected to even do this for a concentration ratio range starting at 100 or even below.

Many methods which determine an obviously wrong value for R_s still give accurate values for the additional series resistances $R_{a,low}$ and $R_{a,high}$. So, although not suitable for absolute R_s measurements, this indicates that these methods (which often have the practical advantage of only requiring a single *IV*-curve) would be suitable for relative R_s measurements, for instance to experimentally compare various contact grid configurations.

Acknowledgments

The authors would like to thank Afric S. Meijer for some useful discussions. This work was financially supported by the Dutch Technology Foundation (STW) under project no. 07452.

Appendix A

In this study the temperature sensor was connected next to the cell on the same aluminium carrier and virtually all the incident light was focussed onto the solar cell. Upper limits for the solar cell's heat loss through thermal radiation and convection were calculated to be 0.1 and 2.0 W respectively, which are small compared to the approximately 20 W of light with which the solar cell is irradiated at $C=500$ and are, therefore, neglected. This means that the heat flow through the device can be approximated by the basic heat circuit diagram presented in Fig. A1.

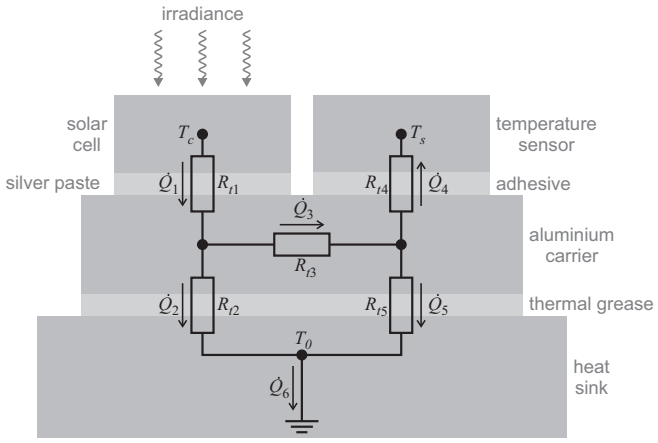

Fig. A1. Schematic representation of the heat flow through the device. Thermal resistance is represented by R_t to avoid any confusion with electrical resistance. Note that the dimensions are not to scale.

At thermal equilibrium $\dot{Q}_4 = 0$, since heat loss through radiation and convection is negligible, so $\dot{Q}_6 = \dot{Q}_1$. Together with the fact that $R_{t5} = R_{t2}$, this means

$$T_c = T_s + \left(R_{t1} + \frac{R_{t2}R_{t3}}{2R_{t2}+R_{t3}}\right)\dot{Q}_1. \tag{A.1}$$

$\dot{Q}_1$ is the heat inserted into the solar cell per unit time and so is proportional to $(1-\eta)C$, where η is the efficiency of the solar cell. Since the variation in $1-\eta$ with C will be relatively small, the relation between T_c, T_s and C can be expressed as

$$T_c = T_s + gC, \tag{A.2}$$

with g a constant. Alternatively, one can write

$$\Delta T_c = \Delta T_s + gC, \tag{A.3}$$

with $\Delta T_{c/s}$ defined as $T_{c/s} - 25$ K. This means that the cell temperature exceeds the sensor temperature, and that the difference is proportional to the concentration ratio.

References

[1] A.R. Moore, An optimized grid design for a sun-concentrator solar cell, RCA Rev. 40 (1979) 140–152.
[2] M.A. Green, Solar Cells: Operating Principles, Technology, and System Applications, Prentice Hall, Englewood Cliffs, 1982.
[3] C. Algora, V. Díaz, Influence of series resistance on guidelines for manufacture of concentrator p-on-n GaAs solar cells, Prog. Photovolt. Res. Appl. 8 (2000) 211–225.
[4] G.M.M.W. Bissels, M.A.H. Asselbergs, J.J. Schermer, E.J. Haverkamp, N.J. Smeenk, E. Vlieg, A genuine circular contact grid pattern for solar cells, Prog. Photovolt. Res. Appl. 18 (2011) 517–526.
[5] P. Mialhe, A. Khoury, J.P. Charles, A review of techniques to determine the series resistance of solar cells, Phys. Stat. Sol. (a) 83 (1984) 403–409.
[6] M.A. Hamdy, R.L. Call, The effect of the diode ideality factor on the experimental determination of series resistance of solar cells, Solar Cells 20 (1987) 119–126.
[7] A.G. Aberle, S.R. Wenham, M.A. Green, A new method for accurate measurements of the lumped series resistance of solar cells, in: Proceedings of the 23rd IEEE Photovoltaic Specialists Conference, Louisville, 1993, pp. 133—139.
[8] M. Bashahu, A. Habyarimana, Review and test of methods for determination of solar cell series resistance, Renew. Energy 6 (1995) 129–138.
[9] A. Mette, D. Pysch, G. Emanuel, D. Erath, R. Preu, S.W. Glunz, Series resistance characterization of industrial silicon solar cells with screen-printed contacts using hotmelt paste, Prog. Photovolt: Res. Appl. 15 (2007) 493–505.
[10] D. Pysch, A. Mette, S.W. Glunz, A review and comparison of different methods to determine the series resistance of solar cells, Solar Energy Mater. Solar Cells 91 (2007) 1698–1706.
[11] G.M.M.W. Bissels, J.J. Schermer, M.A.H. Asselbergs, E.J. Haverkamp, P. Mulder, G.J. Bauhuis, E. Vlieg, Theoretical review of series resistance determination methods for solar cells, 2014, under review.
[12] P.P. Altermatt, G. Heiser, A.G. Aberle, A. Wang, J. Zhao, S.J. Robinson, S. Bowden, M.A. Green, Minimization of resistive losses in high-efficiency Si solar cells, Prog. Photovolt: Res. Appl. 4 (1996) 399–414.

[13] M. Warashina, A. Ushirokawa, Simple method for the determination of series resistance and maximum power of solar cell, Jpn. J. Appl. Phys. 19 (1980) 179–182.
[14] G.L. Araujo, E. Sánchez, A new method for experimental determination of the series resistance of a solar cell, IEEE Trans. Electron Devices 10 (1982) 1511–1513.
[15] M. Wolf, H. Rauschenbach, Series resistance effects on solar cell measurements, Adv. Energy Convers. 3 (1963) 455–479.
[16] L.D. Swanson, Personal communication with Wolf and Rauschenbach, see ref. [15].
[17] P. Mialhe, J. Charette, Experimental analysis of *I–V* characteristics of solar cells, Am. J. Phys. 51 (1983) 68–70.
[18] W.T. Picciano, Determination of the solar cell equation parameters, including series resistance, from empirical data, Energy Convers. 9 (1969) 1–6.
[19] Q. Jia, W.A. Anderson, E. Liu, S. Zhang, A novel approach for evaluating the series resistance of solar cells, Solar Cells 25 (1988) 311–318.
[20] M.A.H. Asselbergs, G.M.M.W. Bissels, G.J. Bauhuis, P. Mulder, J.J. Schermer, E. Vlieg, A laser-based solar simulator for high-precision concentrator cell analysis, 2014, submitted for publication.
[21] G.M.M.W. Bissels, M.A.H. Asselbergs, G.J. Bauhuis, P. Mulder, E.J. Haverkamp, E. Vlieg, J.J. Schermer, Anomalous *IV*-characteristics of a GaAs solar cell under high irradiance, Solar Energy Mater. Solar Cells 104 (2012) 97–101.
[22] H. Helmers, M. Schachtner, A.W. Bett, Influence of temperature and irradiance on triple-junction solar subcells, Solar Energy Mater. Solar Cells 116 (2013) 144–152.
[23] G.L. Araújo, A. Cuevas, J.M. Ruiz, The effect of distributed series resistance on the dark and illuminated current–voltage characteristics of solar cells, IEEE Trans. Electron Devices 33 (1986) 391–401.
[24] R.R. King, D. Bhusari, A. Boca, D. Larrabee, X.-Q. Liu, W. Hong, C.M. Fetzer, D. C. Law, N.H. Karam, Band gap-voltage offset and energy production in next-generation multijunction solar cells, Prog. Photovolt: Res. Appl. 19 (2010) 797–812.
[25] IEC Standard 60891, Procedures for temperature and irradiance corrections to measured *I–V* characteristics of crystalline silicon photovoltaic devices, 1987.